JACS
JOURNAL OF THE AMERICAN CHEMICAL SOCIETY
pubs.acs.org/JACS
Communication

Enhancing the Understanding of Hydrogen Evolution and Oxidation Reactions on Pt(111) through Ab Initio Simulation of Electrode/Electrolyte Kinetics

Ling Liu, Yuyang Liu, and Chungen Liu*

Cite This: J. Am. Chem. Soc. 2020, 142, 4985−4989
Read Online
ACCESS | Metrics & More | Article Recommendations | Supporting Information

ABSTRACT: The hydrogen oxidation reaction (HOR) and hydrogen evolution reaction (HER) play an important role in hydrogen-based energy conversion. However, the sluggish kinetics in alkaline media has raised debates on the relevant mechanism, especially on the role of surface hydroxyl (OH*). With the potential-related free energy profiles obtained with density functional theory calculations, the full pH range transient kinetics simulation of HER/HOR polarization curves on Pt(111) agrees well with experimental observations. Studying model systems with varying metal−OH* binding energies confirms that the current near the HOR onset potential is contributed from the pathway through OH^- rather than OH*, suggesting that OH* is unlikely an effective activity descriptor for HOR. The degree of rate control analyses reveal that, while acidic current is controlled solely by the Tafel step, alkaline current is controlled jointly by Tafel and Volmer steps, as the Volmer barrier is considerably increased in alkaline conditions. Finally, based on a model study, we draw up a scheme of reducing the overpotential of alkaline HER/HOR by accelerating the Tafel step.

Downloaded via SOOCHOW UNIV on May 23, 2023 at 21:24:47 (UTC).
See https://pubs.acs.org/sharingguidelines for options on how to legitimately share published articles.

A promising direction of utilizing the hydrogen energy is through combining water electrolysis and the hydrogen fuel cell. The hydrogen evolution reaction (HER) and hydrogen oxidation reaction (HOR) are two relevant electrochemical reactions in an aqueous environment. Although platinum and its group metals rank among the most active electrocatalysts for HER/HOR, the sluggish kinetics in alkaline conditions has hindered their application in alkaline electrolyzers and anion exchange membrane fuel cells.[1,2] Much effort has been devoted to explore the pH-dependent activity in the HER/HOR system, leading to diverse explanations. The dramatic pH effect has been rationalized as the difficulty in water dissociation,[3,4] the varying transport rate of H^+/OH^-,[5,6] or the shifting of apparent hydrogen binding energy (HBE).[7,8] The activity descriptor for alkaline HOR/HER has not been unambiguously determined either. As HBE is known as the sole descriptor for HER/HOR processes in an acidic environment,[9−11] the adsorbed OH* was suggested as either the second descriptor for the alkaline mechanism[3,12,13] or an inhibitor blocking the active sites.[14−16] Contrarily, much less theoretical work has been directed toward the understanding of the alkaline mechanism, which should reveal the inherent reasons underlying the alkaline activity at the atomic level.

Previous kinetics analyses directed toward the HER/HOR systems were mostly based on simplified reaction models.[3,17−19] Further mechanism exploration was hindered either by the lack of detailed knowledge about the elementary steps or by the invalid assumption of fast equilibrium of Volmer steps for alkaline conditions. Recently, the development of theoretical methods in calculating the potential-related activation barriers in an electrochemical interface has made great progress,[20−24] which has been combined with the microkinetics simulations to offer a reliable tool of verifying the proposed mechanisms and an in-depth exploration of the reaction characteristics.[25−27]

To clarify the ongoing debates, we present here the first multiscale simulation of HER/HOR polarization curves for the full pH range on Pt(111) by solving the integrated equations of the diffusion layer particle transport and the metal/electrolyte interfacial microkinetics. The potential-related kinetics parameters of the surface elementary steps are computed with our previously proposed scheme.[28] The free energies are evaluated with the density functional theory (DFT), while the potential and solvation effects are approximated by the implicit solvation model implemented in VASPsol.[29,30] Additional corrections are introduced to correct the solvation errors[31] and the reported size dependence of the free energy.[32] A brief introduction to the computational methods and a complete collection of the kinetic parameters, as well as the details of results, are available in the SI.

Figure 1 shows all elementary steps considered in constructing the competing acidic and alkaline mechanisms. The potential-dependent reaction free energy and activation barrier for each elementary step are shown in Tables S2 and S3. The coverage effect of surface hydrogen is considered by simulating the electrochemical reactions on clean and 10/12 monolayer (ML) H_f* occupied Pt(111) surfaces, respectively.

Received: December 19, 2019
Published: March 4, 2020

© 2020 American Chemical Society

https://dx.doi.org/10.1021/jacs.9b13694
J. Am. Chem. Soc. 2020, 142, 4985−4989

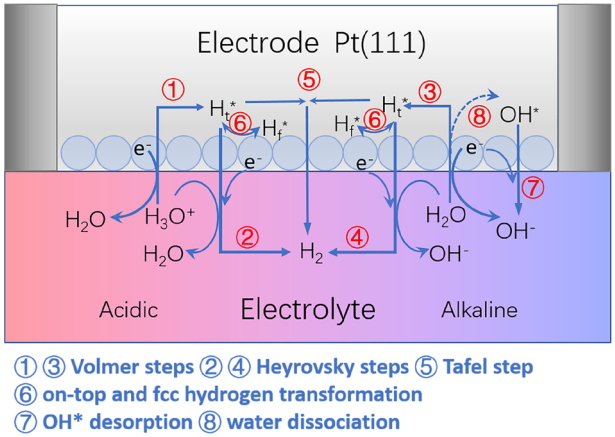

Figure 1. Elementary steps included in the HER/HOR kinetics modeling.

The calculated free energy diagrams for two well-known pathways, Volmer–Heyrovsky and Volmer–Tafel, are presented in Figure S2, which shows the prevailing of the Volmer–Tafel route in the studied pH range at the thermodynamic potentials.

The simulated current–potential polarization curves displayed in Figure 2a agree well with the experimental results

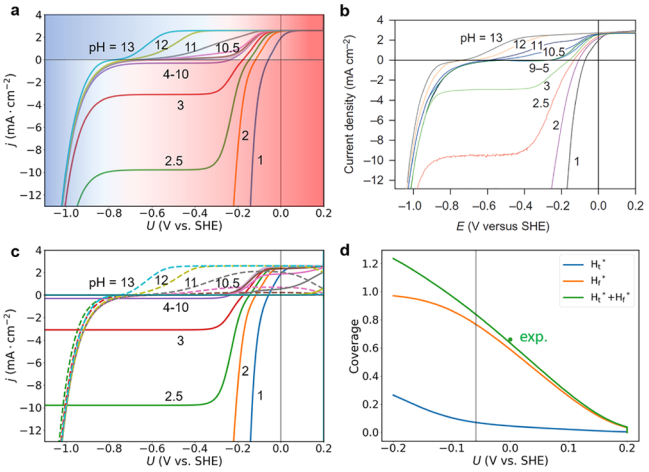

Figure 2. (a) Simulated current–potential polarization curves on Pt(111). (b) Experimental current–potential polarization curves on Pt(111). Reprinted with permission from ref 3. Copyright 2013, Springer Nature. (c) Partial current densities for acidic (full line) and alkaline (dashed line) mechanisms. (d) Plot of the hydrogen coverage vs potential at pH 1.

from Markovic's group (Figure 2b).[3] The total current curves are roughly divided into acidic and alkaline mechanism districts, which are distinguished with graduated red to blue shadows. Figure 2c presents the partial currents of acidic and alkaline mechanisms for a better comparison. In the HER region, the acidic currents (pH 1–4) clearly show a pH-dependent feature, with the following plateau characterizing the H^+ diffusion limit. Contrarily, the alkaline current branch is insensitive to the pH conditions, since the reactant H_2O is assumed as constant. In the HOR region, the pH-independent plateau around 2 mA/cm^2 is attributed to the diffusion control of H_2, while the expected plateau for the OH^--limited transport which should have appeared below pH 11 is absent, as a result of the intervention of acidic HOR currents. It can also be seen that the total HER currents in the alkaline districts for pH 1–4 and the HOR current in the acidic districts for pH 10–11 are jointly contributed from both acidic and alkaline mechanisms.

Figure 2d presents a linear relationship between the total hydrogen coverage and the applied potential at pH 1, which is ca. 0.63 ML at 0 V vs SHE, compared to the experimental value of 0.66 ML.[15] As H_f* is found to be more stable than H_t* (within 0.1 eV), it predominates in the hydrogen adsorption in the HOR region; thereby the HER process is initiated on the surface highly covered with H_f* (ca. 0.77 ML). Due to the limited vacancy for H_f* adsorption, the coverage of H_t* that formed from the H_3O^+ reduction increases superlinearly with the negatively increasing potential, which shows a good agreement with the near-exponential growth of infrared (IR) absorption spectra of H_t*.[33]

The concept of the degree of rate control (DRC) was developed by Campbell to quantify the impact of the free energy perturbation δG_i of a specific species i on the total reaction rate, which has been widely adopted to identify the rate-controlling transition states (TS) and intermediates.[34] For the convenience in electrochemistry, we slightly modify the original DRC equation to express the degree of control on current density j:

$$\mathrm{DRC}_i = -\frac{RT}{j}\left(\frac{\partial j}{\partial G_i}\right)_{G_{k\neq i}} = -RT\left(\frac{\partial \ln|j|}{\partial G_i}\right)_{G_{k\neq i}} \quad (1)$$

The DRCs for transition states are usually positive values (Figure 3a and b), which means stabilizing a TS will increase

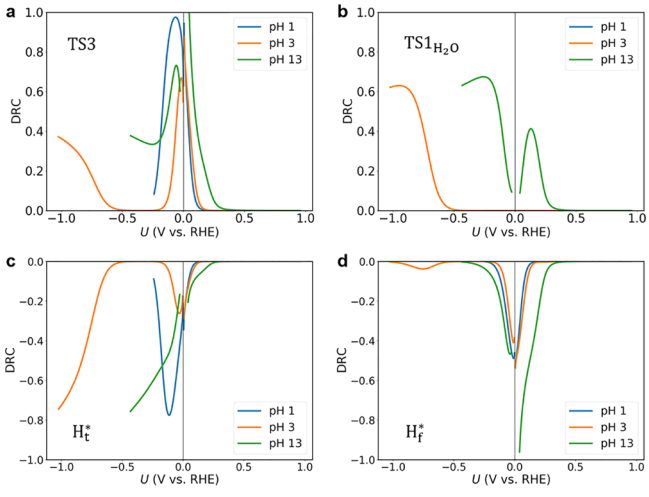

Figure 3. DRC curves for the key species in HER/HOR on Pt(111), including two transition states in (a) Tafel and (b) alkaline Volmer steps and two intermediates, (c) on-top H_t* and (d) fcc H_f*. DRC plots with negligible values for the remaining species are presented in Figure S5.

the current density. Contrarily, stabilizing an intermediate will often slow down the reaction, corresponding to a negative value (Figure 3c and d). DRC analysis allows us to extract the information on current-limiting species from the very complicated kinetics equations and quantify their influences throughout the operation ranges of potential and pH. Technically, each DRC_i is computed with the finite-difference method, setting δG_i as 0.001 eV.

https://dx.doi.org/10.1021/jacs.9b13694
J. Am. Chem. Soc. 2020, 142, 4985–4989

Figure 3a and b illustrate the effects of pH and potential on the DRC of TSs in the Tafel and alkaline Volmer steps. At pH 1 and within small overpotentials, the calculated DRCs of the Tafel step are close to 1.0, indicating an exclusive control on the HER/HOR kinetics, which is in accordance with earlier experimental and theoretical studies.[6,11,35] At pH 3, the zero value of DRCs indicates the H^+ diffusion control in the HER region between −0.2 and −0.5 V vs RHE. Out of this potential range, the HER process follows either an acidic or alkaline mechanism, depending on the potential regions. At alkaline pH, earlier experimental studies of HER/HOR in a H_2-saturated electrolyte on Pt(111) found that the Tafel slope increased continuously with increasing overpotential, so that the rate-determining step (RDS) cannot be unambiguously assigned.[14,36] However, a more recent experimental study suggested the unique control of the Volmer step in the alkaline HER current, according to the Tafel plot obtained under an argon atmosphere, while that in a H_2-saturated electrolyte presented a similar feature to previous experiments.[6] Therefore, the RDS for alkaline HER/HOR remains unclear. Here, the DRC curves for pH 13 show clearly an incomplete transition of the RDS from the Tafel step to the Volmer step, indicating the alkaline HER/HOR current is controlled jointly by both steps in the kinetics-controlled region. In such kind of dual-barrier systems, the apparent activation energy will be related to the applied potential and surface coverage, besides the activation barriers, which explains the observed potential dependence of the Tafel slope.

Analysis on the DRC profiles of H_t* and H_f* reveals their respective roles in controlling the total reaction rate, which can enhance the understanding on the adsorbed hydrogen acting as an activity descriptor in HER/HOR processes. Obviously, DRC values of H_t* in the HER potential region are much larger than that in the HOR region in the whole investigated pH conditions, while those of H_f* behave in an opposite way. This unusual discovery can be rationalized, considering the rapid transformation between H_t* and H_f*. Above the thermodynamic reversible potential, the hydrogen atoms reside predominantly on fcc sites and act as a reactive species in the Volmer step, due to the short lifetime of H_t*. When the overpotentials of HER are applied, a considerable amount of H_t* was produced to take over the role of H_f*, while the latter becomes a spectator on the surface. Therefore, it is interesting to think about the possibility of tuning two kinds of adsorptions with different strategies in optimizing HER/HOR performance.

As shown in Figure 4a and b, two model systems with stronger metal−OH* binding than the Pt(111) surface are computed to look into the role of OH* in alkaline HOR, with the stability of H* remaining invariant. The reaction barriers relevant to OH* are adjusted following the Brønsted−Evans−Polanyi (BEP) principle[37] with a slope of 0.5. Increasing the OH* binding strength is found to impose no effect on the HOR onset potential; instead, it will greatly influence the current-breakdown potential, which is obviously coincident with the desorption potential of OH*. Examination of the OH* coverage (Figure 4a), as well as the partial currents contributed from OH*-mediated and direct OH^- oxidation (Figure 4b), can clearly interpret whether OH* takes part in affecting the kinetics of alkaline HOR. OH* is found to play the role of a reactive species in a certain range of potential, starting from the OH* desorption potential, down to where the direct OH^- oxidation mechanism takes over the OH* mechanism, due to the fast decrease of the OH* coverage and stabilization of TS in the OH^- oxidation step with decreasing potential. Approaching the HOR onset region, the coverage of OH* becomes negligible, together with its influence on HOR kinetics.

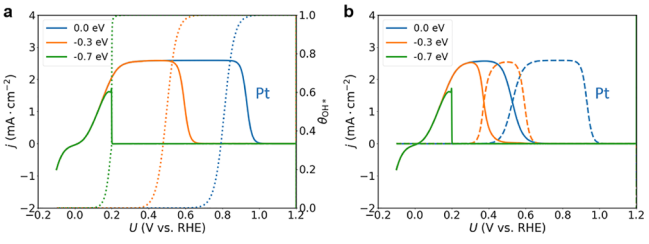

Figure 4. (a) Current−potential polarization curves at pH 13 calculated with varying OH* stabilities. OH* coverage as a function of potential is shown in the dotted curve. (b) Partial current densities for OH* (dashed line) and OH^- (full line) mechanisms.

The above theoretical analyses depend on a simplified model assuming H* binding strength is constant with varying OH* stabilities. In real systems, the stabilities of H* and OH* can be internally correlated. Therefore, the previously reported impact of OH* binding strength on HOR activity might also originate from the concurrently varying stability of H*. In some other systems, taking H* as the sole descriptor has been proved to be effective.[8,38,39] At least for alkaline HOR processes on Pt(111) and systems that share the same mechanism, too strong OH* binding would cause a lower breakdown potential and suppress the current density (Figure 4a), just like the case on a Ru(0001) surface.[3]

Based on the theoretical simulation and DRC analyses, the dramatic difference of kinetic performance between the alkaline and acidic HER/HOR is mainly ascribed to the much higher activation barrier of the alkaline Volmer step. The mechanism switching in the Volmer step can be taken as the breaking of the BEP principle, since the two conditions share the same intermediate state H*, but the activation barrier is obviously different. Similarly, instead of relying on the modulation of HBE, it is helpful to think about optimizing the alkaline HER/HOR activity through stabilizing the TS of the Tafel step and maintaining the H* stability, which could considerably reduce the overpotential, as shown in Figure S8. One possible strategy for stabilizing the TS is to polarize the surface hydrogen couples ($H^{*\delta+}$ + $H^{*\delta-}$ ↔ H_2*) through alloying or introducing surface groups, and a similar approach has been proposed in CO dimerization.[40] Hopefully, we anticipate our investigation of the energetics and kinetics of HER/HOR on Pt(111) can be referenced in designing high-performance catalysts, especially in alkaline media.

■ ASSOCIATED CONTENT

Supporting Information

The Supporting Information is available free of charge at https://pubs.acs.org/doi/10.1021/jacs.9b13694.

Detailed computational schemes for the electrode/electrolyte model, potential-related kinetic parameters, DRC curves for the non-rate-controlled species, free energy diagrams of calculated mechanisms, configurations of optimized structure, calculated DFT energies and potentials (PDF)

https://dx.doi.org/10.1021/jacs.9b13694
J. Am. Chem. Soc. 2020, 142, 4985−4989

AUTHOR INFORMATION

Corresponding Author

Chungen Liu − *Institute of Theoretical and Computational Chemistry, Key Laboratory of Mesoscopic Chemistry of the Ministry of Education (MOE), School of Chemistry and Chemical Engineering, Nanjing University, Nanjing 210023, China;* orcid.org/0000-0001-7839-0799; Email: cgliu@nju.edu.cn

Authors

Ling Liu − *Institute of Theoretical and Computational Chemistry, Key Laboratory of Mesoscopic Chemistry of the Ministry of Education (MOE), School of Chemistry and Chemical Engineering, Nanjing University, Nanjing 210023, China;* orcid.org/0000-0002-1557-7983

Yuyang Liu − *Institute of Theoretical and Computational Chemistry, Key Laboratory of Mesoscopic Chemistry of the Ministry of Education (MOE), School of Chemistry and Chemical Engineering, Nanjing University, Nanjing 210023, China;* orcid.org/0000-0002-0808-0047

Complete contact information is available at: https://pubs.acs.org/10.1021/jacs.9b13694

Notes

The authors declare no competing financial interest.

ACKNOWLEDGMENTS

This work is supported by China NSF (Grant Nos. 21173116, 21473088) and the Special Program for Applied Research on Super Computation of the NSFC-Guangdong Joint Fund (the second phase) under Grant No. U1501501. Part of the computations were performed with the computing resources of the High Performance Computing Center of Nanjing University. C.G.L. would like to thank Profs. Yi Gao, Haibo Ma, and Xinghua Xia for constructive suggestions in refining the manuscript.

REFERENCES

(1) Durst, J.; Siebel, A.; Simon, C.; Hasché, F.; Herranz, J.; Gasteiger, H. A. New insights into the electrochemical hydrogen oxidation and evolution reaction mechanism. *Energy Environ. Sci.* **2014**, *7*, 2255−2260.

(2) Sheng, W.; Gasteiger, H. A.; Shao-Horn, Y. Hydrogen oxidation and evolution reaction kinetics on platinum: Acid vs alkaline electrolytes. *J. Electrochem. Soc.* **2010**, *157*, B1529−B1536.

(3) Strmcnik, D.; Uchimura, M.; Wang, C.; Subbaraman, R.; Danilovic, N.; Van Der Vliet, D.; Paulikas, A. P.; Stamenkovic, V. R.; Markovic, N. M. Improving the hydrogen oxidation reaction rate by promotion of hydroxyl adsorption. *Nat. Chem.* **2013**, *5*, 300−306.

(4) Zheng, Y.; Jiao, Y.; Vasileff, A.; Qiao, S.-Z. The hydrogen evolution reaction in alkaline solution: From theory, single crystal models, to practical electrocatalysts. *Angew. Chem., Int. Ed.* **2018**, *57*, 7568−7579.

(5) Rossmeisl, J.; Chan, K.; Skúlason, E.; Björketun, M. E.; Tripkovic, V. On the pH dependence of electrochemical proton transfer barriers. *Catal. Today* **2016**, *262*, 36−40.

(6) Ledezma-Yanez, I.; Wallace, W. D. Z.; Sebastián-Pascual, P.; Climent, V.; Feliu, J. M.; Koper, M. T. M. Interfacial water reorganization as a pH-dependent descriptor of the hydrogen evolution rate on platinum electrodes. *Nat. Energy* **2017**, *2*, 17031.

(7) Cheng, T.; Wang, L.; Merinov, B. V.; Goddard, W. A. Explanation of dramatic pH-dependence of hydrogen binding on noble metal electrode: Greatly weakened water adsorption at high pH. *J. Am. Chem. Soc.* **2018**, *140*, 7787−7790.

(8) Sheng, W.; Zhuang, Z.; Gao, M.; Zheng, J.; Chen, J. G.; Yan, Y. Correlating hydrogen oxidation and evolution activity on platinum at different pH with measured hydrogen binding energy. *Nat. Commun.* **2015**, *6*, 5848.

(9) Trasatti, S. Work function, electronegativity, and electrochemical behaviour of metals: III. Electrolytic hydrogen evolution in acid solutions. *J. Electroanal. Chem. Interfacial Electrochem.* **1972**, *39*, 163−184.

(10) Nørskov, J. K.; Bligaard, T.; Logadottir, A.; Kitchin, J. R.; Chen, J. G.; Pandelov, S.; Stimming, U. Trends in the exchange current for hydrogen evolution. *J. Electrochem. Soc.* **2005**, *152*, J23−J26.

(11) Skúlason, E.; Tripkovic, V.; Björketun, M. E.; Gudmundsdóttir, S.; Karlberg, G.; Rossmeisl, J.; Bligaard, T.; Jónsson, H.; Nørskov, J. K. Modeling the electrochemical hydrogen oxidation and evolution reactions on the basis of density functional theory calculations. *J. Phys. Chem. C* **2010**, *114*, 18182−18197.

(12) Koper, M. T. M. A basic solution. *Nat. Chem.* **2013**, *5*, 255−256.

(13) Strmcnik, D.; Lopes, P. P.; Genorio, B.; Stamenkovic, V. R.; Markovic, N. M. Design principles for hydrogen evolution reaction catalyst materials. *Nano Energy* **2016**, *29*, 29−36.

(14) Schmidt, T.; Ross, P.; Markovic, N. Temperature dependent surface electrochemistry on Pt single crystals in alkaline electrolytes: Part 2. The hydrogen evolution/oxidation reaction. *J. Electroanal. Chem.* **2002**, *524*−*525*, 252−260.

(15) Marković, N. M.; Ross, P. N. Surface science studies of model fuel cell electrocatalysts. *Surf. Sci. Rep.* **2002**, *45*, 117−229.

(16) Intikhab, S.; Snyder, J. D.; Tang, M. H. Adsorbed hydroxide does not participate in the Volmer step of alkaline hydrogen electrocatalysis. *ACS Catal.* **2017**, *7*, 8314−8319.

(17) Asiri, H. A.; Anderson, A. B. Using Gibbs energies to calculate the Pt(111) Hupd cyclic voltammogram. *J. Phys. Chem. C* **2013**, *117*, 17509−17513.

(18) Zhang, Q.; Liu, Y.; Chen, S. A DFT calculation study on the temperature-dependent hydrogen electrocatalysis on Pt(111) surface. *J. Electroanal. Chem.* **2013**, *688*, 158−164.

(19) Karlberg, G. S.; Jaramillo, T. F.; Skúlason, E.; Rossmeisl, J.; Bligaard, T.; Nørskov, J. K. Cyclic voltammograms for H on Pt(111) and Pt(100) from first principles. *Phys. Rev. Lett.* **2007**, *99*, 126101.

(20) Rossmeisl, J.; Skúlason, E.; Björketun, M. E.; Tripkovic, V.; Nørskov, J. K. Modeling the electrified solidliquid interface. *Chem. Phys. Lett.* **2008**, *466*, 68−71.

(21) Chan, K.; Nørskov, J. K. Electrochemical barriers made simple. *J. Phys. Chem. Lett.* **2015**, *6*, 2663−2668.

(22) Goodpaster, J. D.; Bell, A. T.; Head-Gordon, M. Identification of possible pathways for CC bond formation during electrochemical reduction of CO_2: New theoretical insights from an improved electrochemical model. *J. Phys. Chem. Lett.* **2016**, *7*, 1471−1477.

(23) Cheng, T.; Xiao, H.; Goddard, W. A. Full atomistic reaction mechanism with kinetics for CO reduction on Cu100 from ab initio molecular dynamics free-energy calculations at 298 K. *Proc. Natl. Acad. Sci. U. S. A.* **2017**, *114*, 1795−1800.

(24) Xiao, H.; Cheng, T.; Goddard, W. A. Atomistic mechanisms underlying selectivities in C1 and C2 products from electrochemical reduction of CO on Cu(111. *J. Am. Chem. Soc.* **2017**, *139*, 130−136.

(25) Hansen, H. A.; Viswanathan, V.; Nørskov, J. K. Unifying kinetic and thermodynamic analysis of 2 e^- and 4 e^- reduction of oxygen on metal surfaces. *J. Phys. Chem. C* **2014**, *118*, 6706−6718.

(26) Singh, M. R.; Goodpaster, J. D.; Weber, A. Z.; Head-Gordon, M.; Bell, A. T. Mechanistic insights into electrochemical reduction of CO_2 over Ag using density functional theory and transport models. *Proc. Natl. Acad. Sci. U. S. A.* **2017**, *114*, E8812−E8821.

(27) Lamoureux, P. S.; Singh, A. R.; Chan, K. pH effects on hydrogen evolution and oxidation over Pt(111): Insights from first-principles. *ACS Catal.* **2019**, *9*, 6194−6201.

(28) Liu, L.; Liu, C. Origin of the overpotentials for $HCOO^-$ and CO formation in the electroreduction of CO_2 on Cu(211): the reductive desorption processes decide. *Phys. Chem. Chem. Phys.* **2018**, *20*, 5756−5765.

(29) Mathew, K.; Sundararaman, R.; Letchworth-Weaver, K.; Arias, T. A.; Hennig, R. G. Implicit solvation model for density-functional study of nanocrystal surfaces and reaction pathways. *J. Chem. Phys.* **2014**, *140*, 084106.
(30) Mathew, K.; Hennig, R. G. Implicit self-consistent description of electrolyte in plane-wave density-functional theory. 2016, *arXiv*, 1601.03346.
(31) Sundararaman, R.; Schwarz, K. Evaluating continuum solvation models for the electrode-electrolyte interface: Challenges and strategies for improvement. *J. Chem. Phys.* **2017**, *146*, 84111.
(32) Van Den Bossche, M.; Skúlason, E.; Rose-Petruck, C.; Jónsson, H. Assessment of constant-potential implicit solvation calculations of electrochemical energy barriers for H_2 evolution on Pt. *J. Phys. Chem. C* **2019**, *123*, 4116−4124.
(33) Kunimatsu, K.; Uchida, H.; Osawa, M.; Watanabe, M. In situ infrared spectroscopic and electrochemical study of hydrogen electro-oxidation on Pt electrode in sulfuric acid. *J. Electroanal. Chem.* **2006**, *587*, 299−307.
(34) Campbell, C. T. The degree of rate control: A powerful tool for catalysis research. *ACS Catal.* **2017**, *7*, 2770−2779.
(35) Seto, K.; Iannelli, A.; Love, B.; Lipkowski, J. The influence of surface crystallography on the rate of hydrogen evolution at Pt electrodes. *J. Electroanal. Chem. Interfacial Electrochem.* **1987**, *226*, 351−360.
(36) Barber, J.; Conway, B. Structural specificity of the kinetics of the hydrogen evolution reaction on the low-index surfaces of Pt single-crystal electrodes in 0.5 M dm^{-3} NaOH. *J. Electroanal. Chem.* **1999**, *461*, 80−89.
(37) Bligaard, T.; Nørskov, J.; Dahl, S.; Matthiesen, J.; Christensen, C.; Sehested, J. The Brønsted−Evans−Polanyi relation and the volcano curve in heterogeneous catalysis. *J. Catal.* **2004**, *224*, 206−217.
(38) Wang, Y.; Wang, G.; Li, G.; Huang, B.; Pan, J.; Liu, Q.; Han, J.; Xiao, L.; Lu, J.; Zhuang, L. Pt-Ru catalyzed hydrogen oxidation in alkaline media: Oxophilic effect or electronic effect? *Energy Environ. Sci.* **2015**, *8*, 177−181.
(39) Lu, S.; Zhuang, Z. Investigating the influences of the adsorbed species on catalytic activity for hydrogen oxidation reaction in alkaline electrolyte. *J. Am. Chem. Soc.* **2017**, *139*, 5156−5163.
(40) Xiao, H.; Goddard, W. A.; Cheng, T.; Liu, Y. Cu metal embedded in oxidized matrix catalyst to promote CO_2 activation and CO dimerization for electrochemical reduction of CO_2. *Proc. Natl. Acad. Sci. U. S. A.* **2017**, *114*, 6685−6688.

https://dx.doi.org/10.1021/jacs.9b13694
J. Am. Chem. Soc. 2020, 142, 4985−4989